Soft Matter

Accepted Manuscript

ROYAL SOCIETY OF CHEMISTRY

www.rsc.org/softmatter

Quantitative Analogy Between Polymer-Grafted Nanoparticles and Patchy Particles

Makoto Asai,[1] Angelo Cacciuto,[2] Sanat K. Kumar[1]

1. Department of Chemical Engineering, Columbia University, New York, 10027.
2. Department of Chemistry, Columbia University, New York, 10027.

Abstract

We establish a quantitative analogy between polymer grafted nanoparticles (PGNPs) and patchy nanoparticles (NPs). Over much of the experimentally relevant parameter space, we show that PGNPs behave quantitatively like Janus NPs, with the patch size having a universal dependence on the number of grafts and the ratio of the size of the NPs to the grafted chain size. The widely observed anisotropic self-assembly of PGNP into superstructures can thus be understood through simple geometric considerations of single patch models, in the same spirit as the geometry-based surfactant models of Israelachvili.

The anisotropic self-assembly of spherical nanoparticles (NPs) uniformly grafted with polymer chains (PGNPs) [1-6] into a variety of anisotropic morphologies is attributed to the energetic dislike between the NP core and the polymeric tethers. Thus, by analogy of PGNPs to block copolymers and other surfactants [7-20], it follows that various assemblies formed by these PGNPs, such as three-dimensional spherical aggregates, two-dimensional sheets, one-dimensional strings, and well-dispersed morphologies are sensitively controlled by grafting density and the size of grafted polymers (or their chain length) relative to the NP size. While the resulting morphologies are thus thought to be a consequence of the microphase separation between the (hydrophilic) NP cores and (hydrophobic) grafted polymers, a central question is why these NPs form anisotropic assemblies even though the spherical building block NPs are isotropically grafted with polymer chains. Thus, an overarching question is what breaks the inherent spherical symmetry of the building block shapes and interactions and leads to the formation of anisotropic morphologies. Inspired by the experimental finding that NPs only form anisotropic assemblies when they are sparsely tethered with macromolecules,[21] Bozorgui et al.,[22] showed that this result did not arise as a result of competing interactions (i.e., short ranged inter NP attractions balanced against brush induced longer ranged repulsion) or from emergent many-body effects. Rather, this anisotropy was found to be inherently encoded at the single PGNP level, as a consequence of large fluctuations of polymer grafting density on surface of a NP due to the small number statistics. More specifically, computer simulations show that the organization of grafts around an individual NP is not spatially isotropic for small numbers of grafts and ligand monomers[23]. This inherent, spatially asymmetric ligand distribution causes the effective, two-body inter-NP potential to have a strong orientational dependence, which reproduces the anisotropic assembly observed ubiquitously for these systems.

Here, we use this qualitative information to construct a quantitatively accurate coarse-grained model for PGNPs in the limit of sparse grafting, i.e., in the regime where they self-assemble into a variety of anisotropic structures. Unlike our previous work[22], where the extraction of the coarse-grained inter-particle interactions required explicit numerical simulations of PGNPs for every different set of structural parameters defining the nanoparticles, here we develop a procedure to explicitly map PGNPs into an effective patchy particle with one attractive patch (corresponding to core-core attractions) and a repulsive patch (corresponding to the entropic repulsion between the grafted NPs). The result is an analytical and *transferable* potential that has a universal dependence on the

number of grafts and the ratio of the size the nanoparticles to the grafted chains. Strikingly, once the mapping of a PGNP into a single-patch particle is performed, we can use simple geometric arguments to identify the boundaries between the different self-assembled morphologies.

To make progress, we need to model a spherical NP randomly grafted with f freely jointed polymer tethers. To simplify these calculations, we represented the NP as a hard sphere of radius R_n, and replaced each polymeric graft by a grafted sphere (GS) of radius, R. This is a reasonable approximation when the surface is not adsorbing to the chains, and R is directly related to the radius of gyration, R_g of the polymeric grafts. Parenthetically, we note that previous work has established that it is reasonable to model self-avoiding polymers by spheres, so long as the spheres are treated as soft, penetrable entities.[24] It also appears that grafting these chains onto a spherical surface only weakly changes the chain size, i.e., by a factor $f^{1/5}$.[25] The size ratio of the GS to the NP is denoted by α ($\equiv R/R_n$). The presence of a single graft excludes a certain fraction of the NP surface, γ^* (related to the solid angle $2\theta_c$), to any other NP, Fig. 1(a). From simple geometric considerations it follows that $cos\theta_c = (1+\alpha)^{-1}$, from which $\gamma^* = (1 - cos\theta_c)/2 = \alpha(1+\alpha)^{-1}/2$. When the distance between two GSs is nearer than the situation shown in Fig. 1(b), then the "covered" areas of two GSs overlap, and these two grafts are part of the same cluster of "covered" areas.

To quantify the fraction of the surface that is occluded by the GS, as well as to obtain the distribution of clusters of covered areas as a function of α and f, we considered a single NP, and randomly placed a number of GSs on its surface. Previous work has shown that the soft sphere potential between two GS has an overlap energy of only ~ $2kT$, implying that they are really quite penetrable.[24] We therefore allow the overlap of the GSs in our model. We performed 1000 different realizations for each state point. Fig. 2 plots the total area S of the NP surface that is inaccessible to a second NP core due to the presence of the GS driven excluded area clusters, normalized by the total NP surface area, $S^* \equiv S/4\pi R_n^2$, as a function of $\gamma^* f$. (In independent work we have shown that $\gamma^* f$ is proportional to the maximum number of chains that can be grafted to the NP surface.) To quantify S^* we place the desired number of grafts on the NP surface. We first tessellate the surface of the NP into 12002 points placed at the vertices of a spherical crystal following the symmetry of a (20, 20) icosadeltahedron. Then, we choose one of these points and place a second bare NP so that its center is exactly one diameter from

the center of the first NP and the line joining the centers of the two NPs passes through this surface point. If the second NP interacts with a GS, then the position is regarded as "covered". We repeat this procedure over the whole surface. It is immediately evident that the S^* from all α values collapse onto the same universal plot (Fig. 2). To understand this apparently universal behavior, we consider the quantity $dS^*/d(f\gamma^*)$ which expresses the change in S^* with the addition of grafts. We adopt ideas analogous to random sequential adsorption [26] and write:

$$\frac{dS^*}{d(f\gamma^*)} = (1 - S^*) \qquad (1)$$

That is, we postulate that the "covered" surface area can only increase if the newly added GS falls on the previously uncovered part of the surface. This yields: $S^* = 1 - e^{-f\gamma^*}$ which is in excellent agreement with our simulation results, indicating that we have a means of quantitatively describing the surface coverage of the grafts on the NP surface with variations in f and α. While this result is encouraging it is unclear whether these grafts form a single cluster ("single patch") or there are multiple clusters of excluded area on the NP surface. We probe this critical question next.

We enumerated the average number of clusters, N_{cl}, over a broad range of f and α [Fig. 3(a)]. For each α, with increasing f, the number of clusters grows from unity, goes through a maximum and eventually returns to unity. Fig. 3(b) then plots the maximum number of clusters, N_{max}, as a function of α. We find that N_{max} decreases rapidly with increasing α, and for the practically relevant cases where $\alpha > 0.3$ the maximum number of clusters is always less than 2. This indicates that there is practically only a single cluster in most cases, a point we shall elaborate on below. For smaller α, a situation that has not been vigorously explored experimentally, the surface typically has multiple clusters.

We now examine the cluster size distributions for different α at N_{max} in Fig. 3(c). First, let us consider the practically significant cases with α= 0.4 and 0.6. We find very narrow distributions, with predominantly single clusters being the norm. For comparison, when $\alpha < 0.3$, we find that the distributions are broader, indicating the presence of several clusters. Our results strongly support the idea that low density PGNPs with $\alpha \geq 0.3$ behave akin to Janus particles [27], with one attractive and one repulsive patch on the NP surface. Such an analogy is powerful since there are now

many works in the literature that have examined the physical properties and the self-assembly of patchy colloids [28-31]. Indeed, Chen et al., have shown that patchy particles could form novel crystalline structures, which were totally different from conventional morphologies formed by isotropic colloids [32].

The most important test of this coarse-graining methodology is to check whether we can predict the self-assembled structures formed by PGNPs. For simplicity, we assume that the PGNP repulsive region can be represented by a single "spherical cap" patch, which covers a fractional area S^* of the surface. As noted above, we assume that there is a strong attraction between the NP cores, but a brush-induced entropic repulsion for any interaction involving a patch created by surface areas that are excluded by the presence of the grafts. Thus, the interaction between two patches or between a patch and a core is assumed to be repulsive. With these assumptions, it is apparent that two NPs cannot approach each other when $S^* \to 1$. The result is a solution with well-dispersed NP. Upon decreasing S^*, when a sufficiently large attractive area is exposed so that at least two NP can come together, *clump*s begin to form.

To derive this boundary we use simple geometric arguments. The angle, $2\theta_{cl-d}$ in Fig. 4(a) is defined as $2\pi - \angle$BOD, and can be expressed as $2\theta_{cl-d} = 2\pi - 2\angle\text{AOC} + 2\angle\text{AOB}$. Here, $\angle$AOB corresponds to what we defined as θ_c, i.e. the angle spanning the fraction of particle surface excluded to other NPs by a single GS. As illustrated in Fig. 1(a), $2\theta_c$ is obtained by tracing two lines tangent to a NP surface that simultaneously pass through the center of the GS. The smallest angle defining the arc connecting the two tangent points is $2\theta_c$. To obtain $\angle$AOC, denoted by θ_0, we use the similar triangles ΔOHF and ΔGHI. This results in $\theta_0 = cos^{-1}\left(\frac{1-\alpha}{1+\alpha}\right)$, and finally $S^*_{cl-d} = \frac{1-cos\theta_{cl-d}}{2} = \frac{1}{2}\{1 - \cos(\pi - \theta_0 + \theta_c)\} = \frac{1}{2}\left[1 - \cos\left\{\pi - cos^{-1}\left(\frac{1-\alpha}{1+\alpha}\right) + cos^{-1}(1-2\gamma^*)\right\}\right]$. A further decrease in S^*, takes us to a region where NPs are able to connect side by side with their repulsive regions oriented opposite to each other. Here, linear aggregates (strings) will form. The string-clump boundary can be identified by imposing the condition represented in Fig. 4(b). Using analogous geometrical arguments as the ones discussed above, one obtains $S^*_{st-cl} = \frac{1-cos\theta_{st-cl}}{2} = \frac{1}{2}$. For even smaller values of S^*, NPs are able to locally arrange into two dimensional structures (sheets) by connecting laterally and from below to form

bilayer sheets that maximize their polymer-free surface contacts. This condition is met when S^* is smaller than $S^*_{sh-st} = \frac{1-cos\theta_{sh-st}}{2} = \frac{1}{2}\left[1 - cos\left\{\frac{\pi}{2} - cos^{-1}\left(\frac{1-\alpha}{1+\alpha}\right) + cos^{-1}(1 - 2\gamma^*)\right\}\right]$ (see Fig. 4(c)), and establishes the sheet-string boundary. The last dividing-line is between three dimensional aggregates and sheets (aggregate-sheet). This occurs when the repulsive regions can be buried in the interstitial spaces between the NPs in their close-packed configuration as shown in Fig. 4(d). This condition is met as soon as $S^*_{ag-sh} = \frac{1-cos\theta_{ag-sh}}{2} = \frac{1}{2}\left[1 - cos\left\{\frac{\pi}{4} - cos^{-1}\left(\frac{1-\alpha}{1+\alpha}\right) + cos^{-1}(1 - 2\gamma^*)\right\}\right]$. Since we have a universal dependence for S^* as a function of f, we can convert these boundaries into a plot of f vs. α.

To confirm the underlying assumptions in our coarse-graining procedure, especially the one that we can model PGNPs as single patch colloids, we compared these geometrically derived boundaries between different morphologies with the recent results of Akcora et al. [1]. Akcora et al. used a model that explicitly accounted for the grafted chains, and used computer simulations to derive a "morphology diagram", Fig. 5, that is in good agreement with experimental results. Before we can place our boundaries over this diagram, we need to relate the size of the GSs to the length of the grafted chains. However, the strong finite size effects inherent in our physical system make this mapping not so straightforward. Indeed, the measured radius of gyration R_g of a single tethered chain (modeled as a sequence of N hard spheres linearly connected by harmonic springs) grafted to the NP results in $R_g \approx aN^{\nu}$ with $\nu \approx 0.73$ and $a \approx 0.32$ for $N \leq 15$ (data not shown). The deviation from the known Flory exponent (0.588) is clearly the combined effect of grafting and short chain sizes, and indeed we find that Flory scaling is obtained asymptotically for chains $N \geq 20$. We therefore do not expect a one-to-one relation between R and R_g, and we postulate that $R = \beta R_g$ and treat β as an adjustable parameter. Fig 5 shows that $\beta = 0.46$ allows us to quantitatively describe all of the data from Akcora et al., except for small deviations in the boundary between sheets and spherical clusters. We believe that this minor disagreement reflects the fact that this boundary is in the limit where the PGNP do not behave akin to a single patch colloid, but rather a colloid with multiple patches.

Importantly, our results provide a powerful tool for the quantitative description of

PGNPs. Not only do we show how PGNP can be mapped into a single patch colloid, and how the size of the patch, S^*, can be derived in a universal manner (Fig. 2), but we also provide simple geometric ideas to derive the boundaries between the different self-assembled morphologies assumed by PGNPs. These results suggest that the physics of these PGNPs are completely analogous to Janus colloids.

The authors thank the National Science Foundation for financial support of this work.
AC acknowledges financial supported from the National Science Foundation under CAREER Grant No. DMR-0846426.

References

1. P. Akcora, H. Liu, S. K. Kumar, J. Moll, Y. Li, B. C. Benicewicz, L. S. Schadler, D. Acehan, A. Z. Panagiotopoulos and V. Pryamitsyn, *Nature materials*, 2009, **8**, 354-359.
2. D. Bedrov, G. D. Smith and L. W. Li, *Langmuir*, 2005, **21**, 5251-5255.
3. J. B. Hooper, D. Bedrov and G. D. Smith, *Langmuir*, 2008, **24**, 4550-4557.
4. B. Gao, G. Arya and A. R. Tao, *Nature Nanotechnol.*, 2012, **7**, 433-437.
5. Z. Quan, W. S. Loc, C. Lin, Z. Luo, K. Yang, Y. Wang, H. Wang, Z. Wang and J. Fang, *Nano Lett.*, 2012, **12**, 4409-4413.
6. V. Padmanabhan, *J. Chem. Phys.*, 2012, **137**, 094907.
7. S. C. Glotzer and M. J. Solomon, *Nature Mater.*, 2007, **6**, 557-562.
8. C. R. Iacovella, *Phys. Rev. E*, 2007,, **75**, 040801.
9. F. W. Starr, J. F. Douglas and S. C. Glotzer, *J. Chem. Phys.*, 2003, **119**, 1777-1788.
10. Z. Y. Tang, Z. Zhang, Y. Wang, S. C. Glotzer and N. Kotov, *Science*, 2006, **314**, 274-278.
11. X. Zhang, Z. L. Zhang and S. C. Glotzer, *J. Chem. Phys. C*, 2007, **111**, 4132-4137.
12. Z. L. Zhang, M. A. Horsch, M. H. Lamm and S. C. Glotzer, *Nano Lett.*, 2003, **3**, 1341-1346.
13. A. Stradner, H. Sedgwick, F. Cardinaux, W. C. K. Poon, S. U. Egelhaaf and P. Schurtenberger, *Nature*, 2004, **432**, 492-495.
14. Y. Norizoe and T. Kawakatsu, *Europhys. Lett.*, 2005, **72**, 583-589.
15. Y. Norizoe and T. Kawakatsu, *J. Chem. Phys.*, 2012, **137**, 024904.
16. J. Groenewold and W. K. Kegel, *J. Chem. Phys. B*, 2001, **105**, 11702-11709.
17. M. Grousson, G. Tarjus and P. Viot, *Phys. Rev. E*, 2000, **62**, 7781-7792.
18. S. Mossa, F. Sciortino, P. Tartaglia and E. Zaccarelli, *Langmuir*, 2004, **20**, 10756-10763.
19. W. M. Gelbart, R. P. Sear, J. R. Heath and S. Chaney, *Faraday Discuss*, 1999, **112**, 299-307.
20. G. Malescio and G. Pellicane, *Nature Mater.*, 2003, **2**, 97-100.
21. S. K. Kumar, N. Jouault, B. Benicewicz and T. Neely, *Macromolecules*, 2013, **46**, 3199-3214.
22. B. Bozorgui, D. Meng, S. K. Kumar, C. Chakravarty and A. Cacciuto, *Nano Letters*, 2013, **13**, 2732-2737.
23. J. M. D. Lane and G. S. Grest, *Phys. Rev. Lett.*, 2010, **104**, 235501
24. A. A. Louis, P. G. Bolhuis, J. P. Hansen and E. J. Meijer, *Phys Rev Lett*, 2000, **85**, 2522-2525.
25. K. Binder and A. Milchev, *Journal of Polymer Science Part B-Polymer Physics*, 2012, **50**, 1515-1555.
26. J. Talbot, G. Tarjus, P. R. Van Tassel and P. Viot, *Colloids and Surfaces a-Physicochemical and Engineering Aspects*, 2000, **165**, 287-324.
27. Z. Zhenli and S. C. Glotzer, *Nano Letters*, 2004, **4**, 1407-1413.
28. F. Sciortino and E. Zaccarelli, *Current Opinion in Solid State and Materials Science*, 2011, **15**, 246-253.

29. E. Bianchi, R. Blaak and C. N. Likos, *Phys. Chem. Chem. Phys.*, 2011, **13**, 6397-6410.
30. S. C. Weber and C. P. Brangwynne, *Cell*, 2012, **149**, 1188-1191.
31. P. Li, S. Banjade, H.-C. Cheng, S. Kim, B. Chen, L. Guo, M. Llaguno, J. V. Hollingsworth, D. K. King, S. F. Banani, P. S. Russo, Q. X. Jiang, N. B. T. and M. K. Rosen, *Nature*, 2012, **483**, 336-340.
32. Q. Chen, S. C. Bae and S. Granick, *Nature*, 2011, **469**, 381-384.

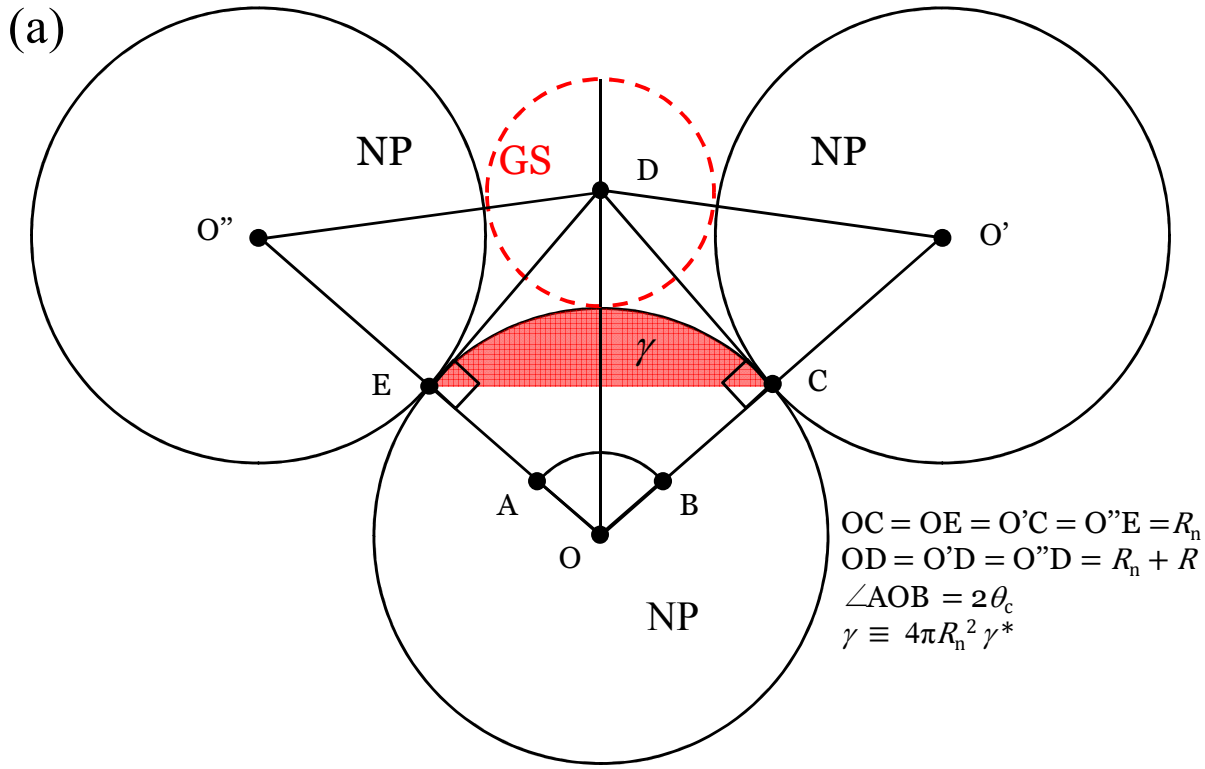

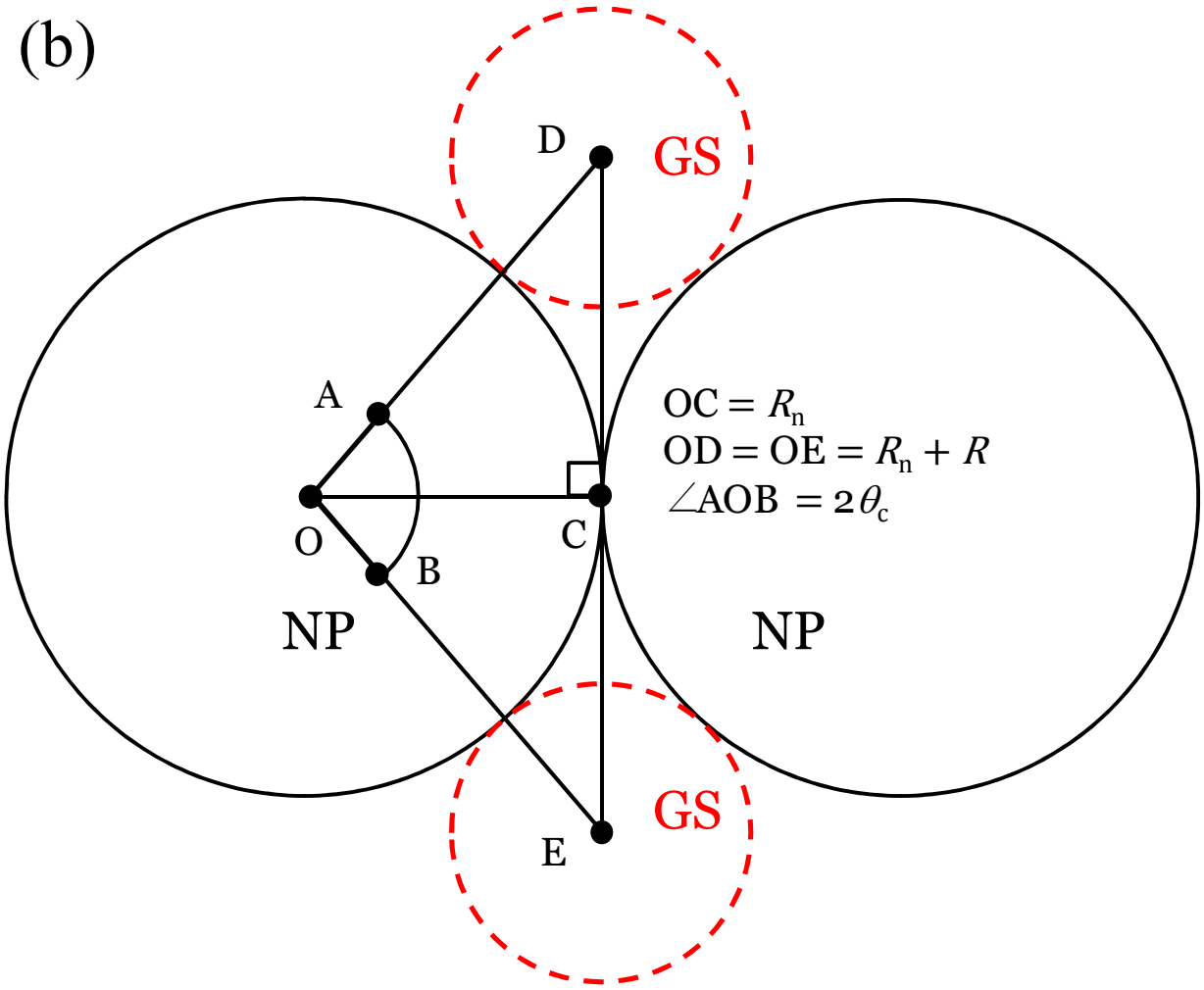

Fig. 1: Geometric representation of our PGNP model. (a) Geometric definition of γ^*, highlighted in red as defined in the text. (b) Geometric definition of a cluster having an angular span of $2\theta_c$. In both figures, R_n is the radius of the nanoparticle and R is the radius the grafted sphere, here represented with a dashed red circle.

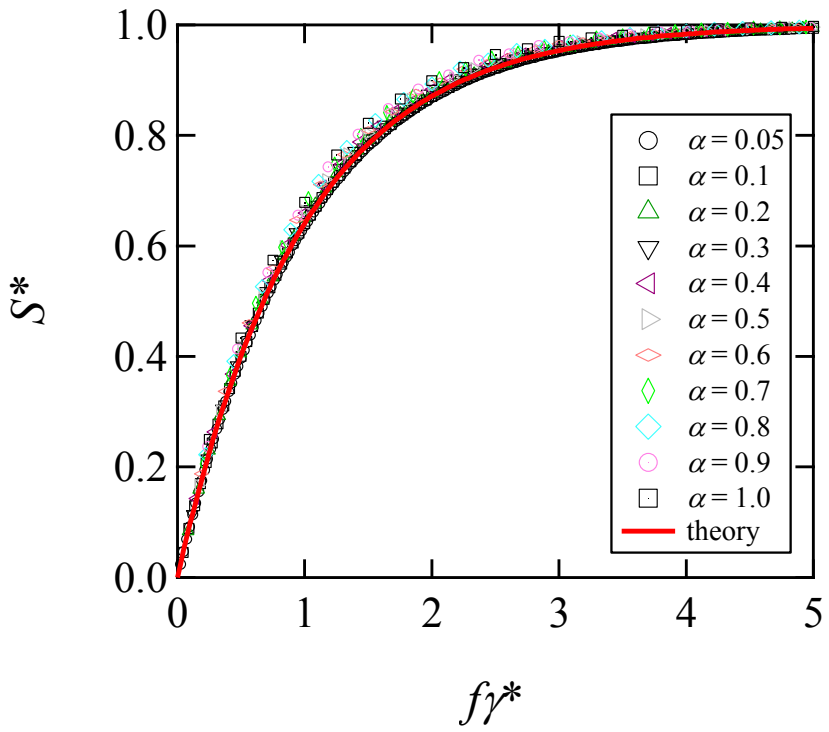

Fig. 2: S^* obtained over a range of f and α values plotted in a form that reduces the data to a universal curve. The solid line represents the theoretical prediction: $S^* = 1 - e^{-f\gamma^*}$.

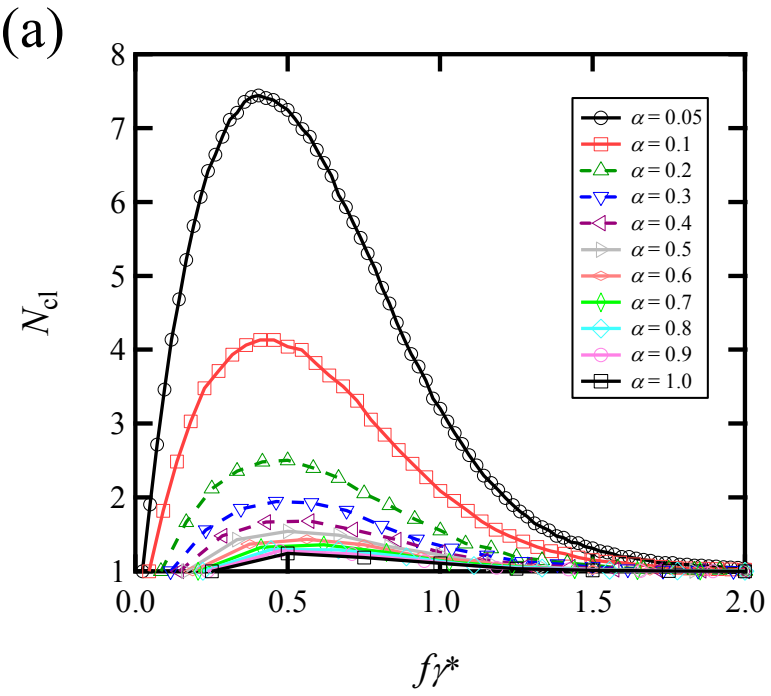

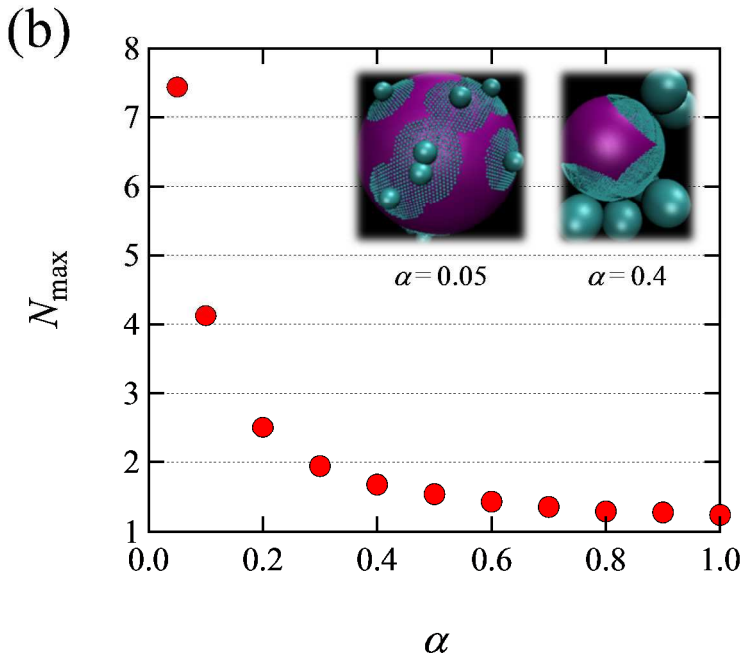

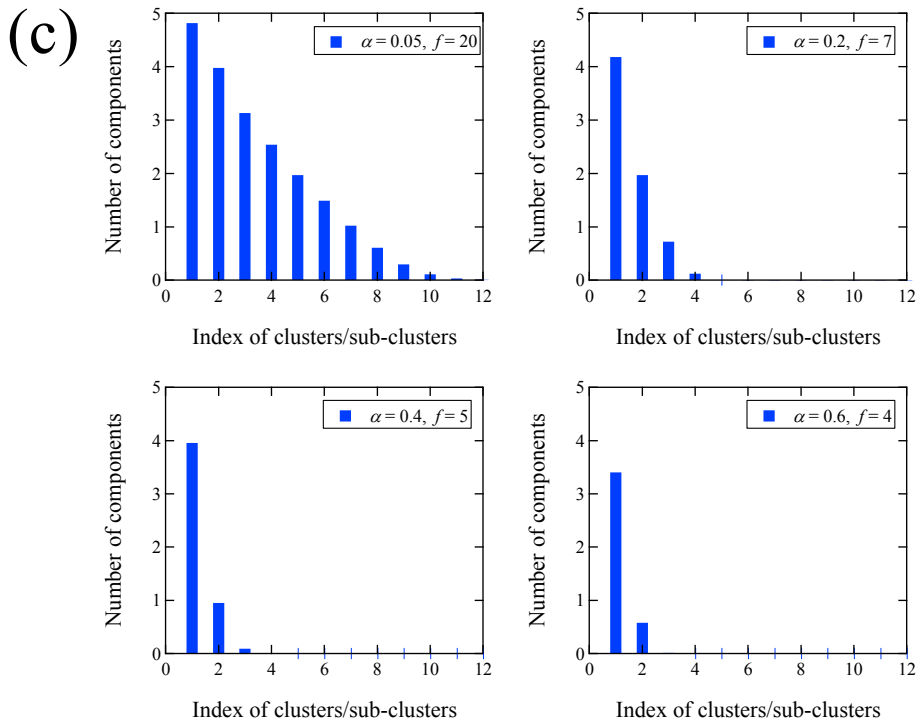

Fig. 3: Cluster analysis. (a) f-dependence of the average number of clusters, N_{cl}, for different values of α. (b) α-dependence of N_{max}, the maximum number of clusters, at each α. Insets show representative snapshots of PGNPs for α = 0.05 and 0.4. NP are colored in purple, GSs and their corresponding covered areas in green (c). Size sorted distribution of the number of grafted polymers in each cluster for different values of α. These distributions are taken for the specific case in which the number of clusters is at its maximum value, $N_{cl} = N_{max}$ for every selected α.

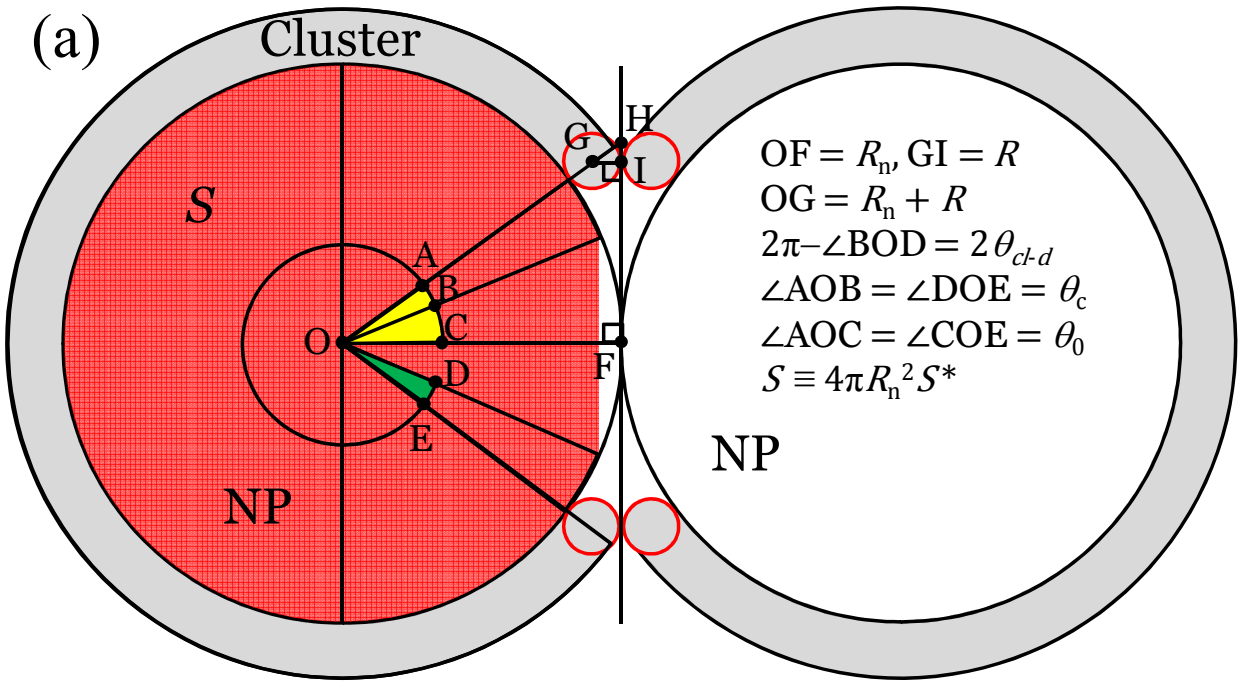

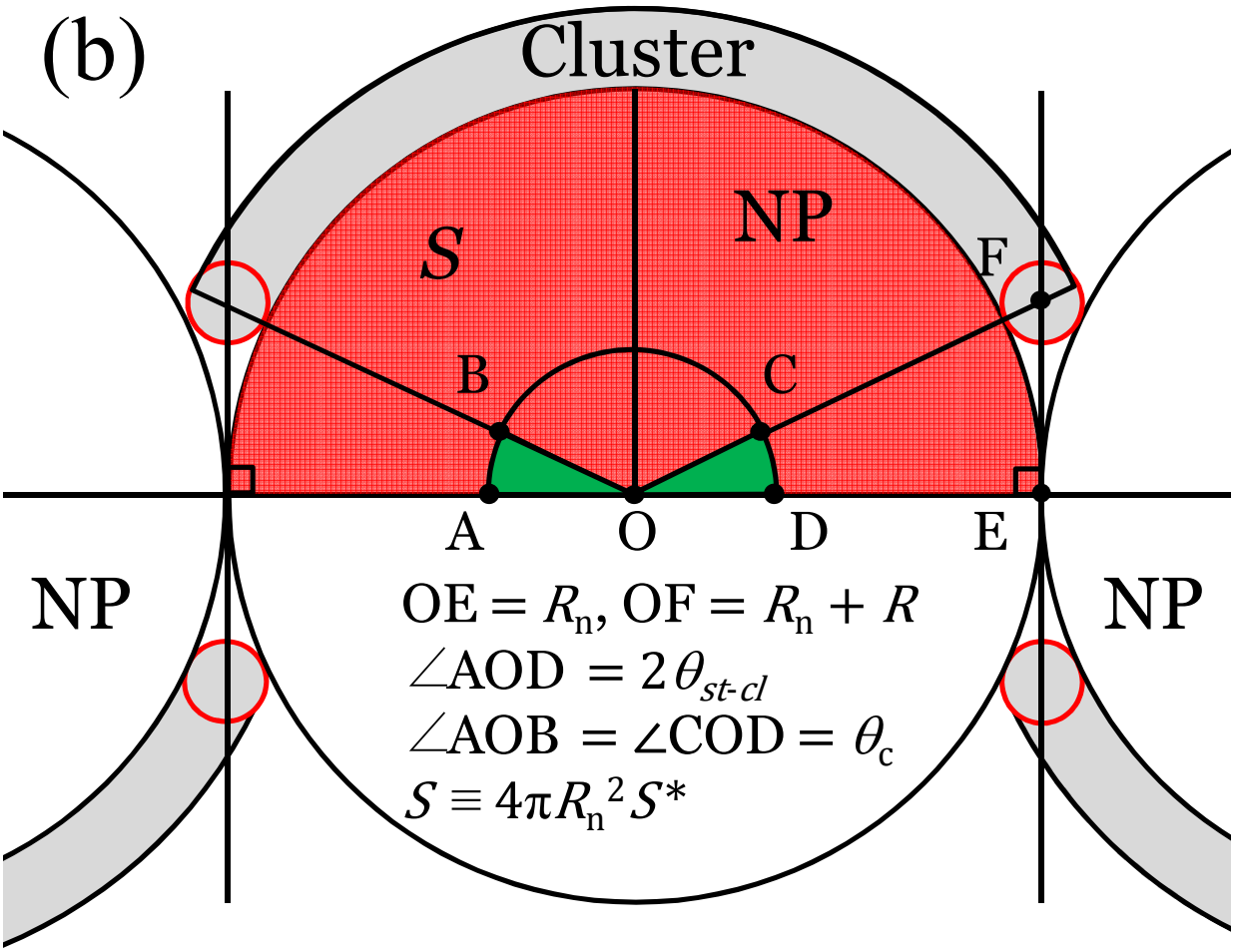

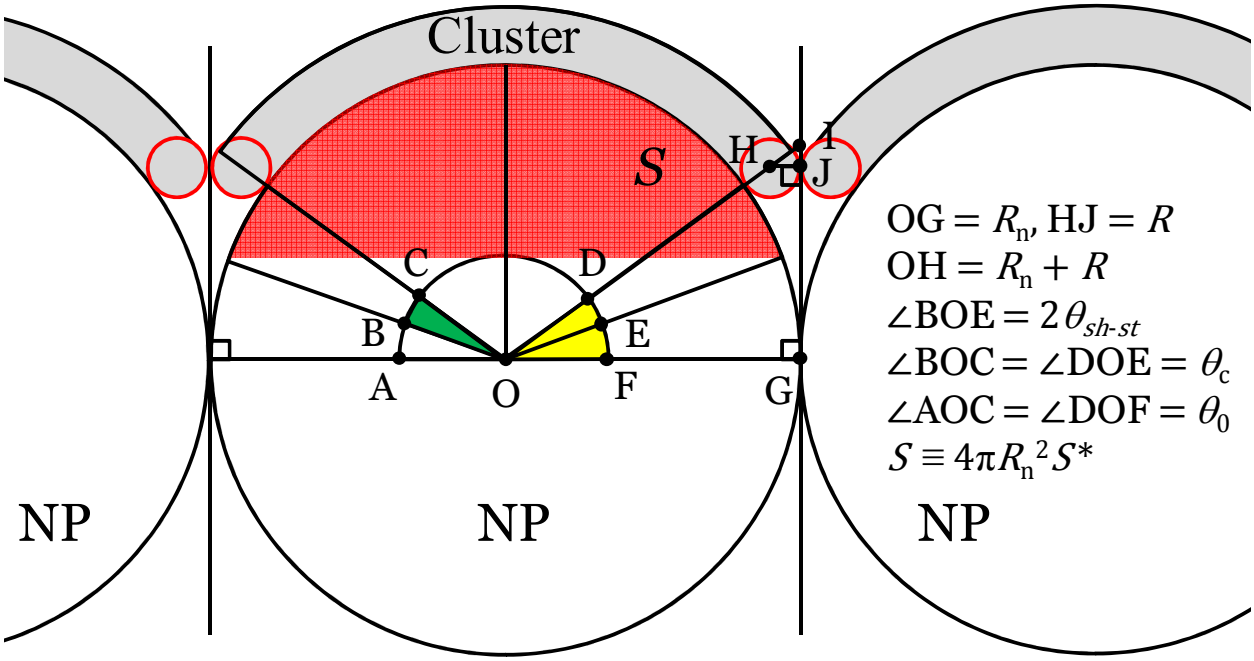

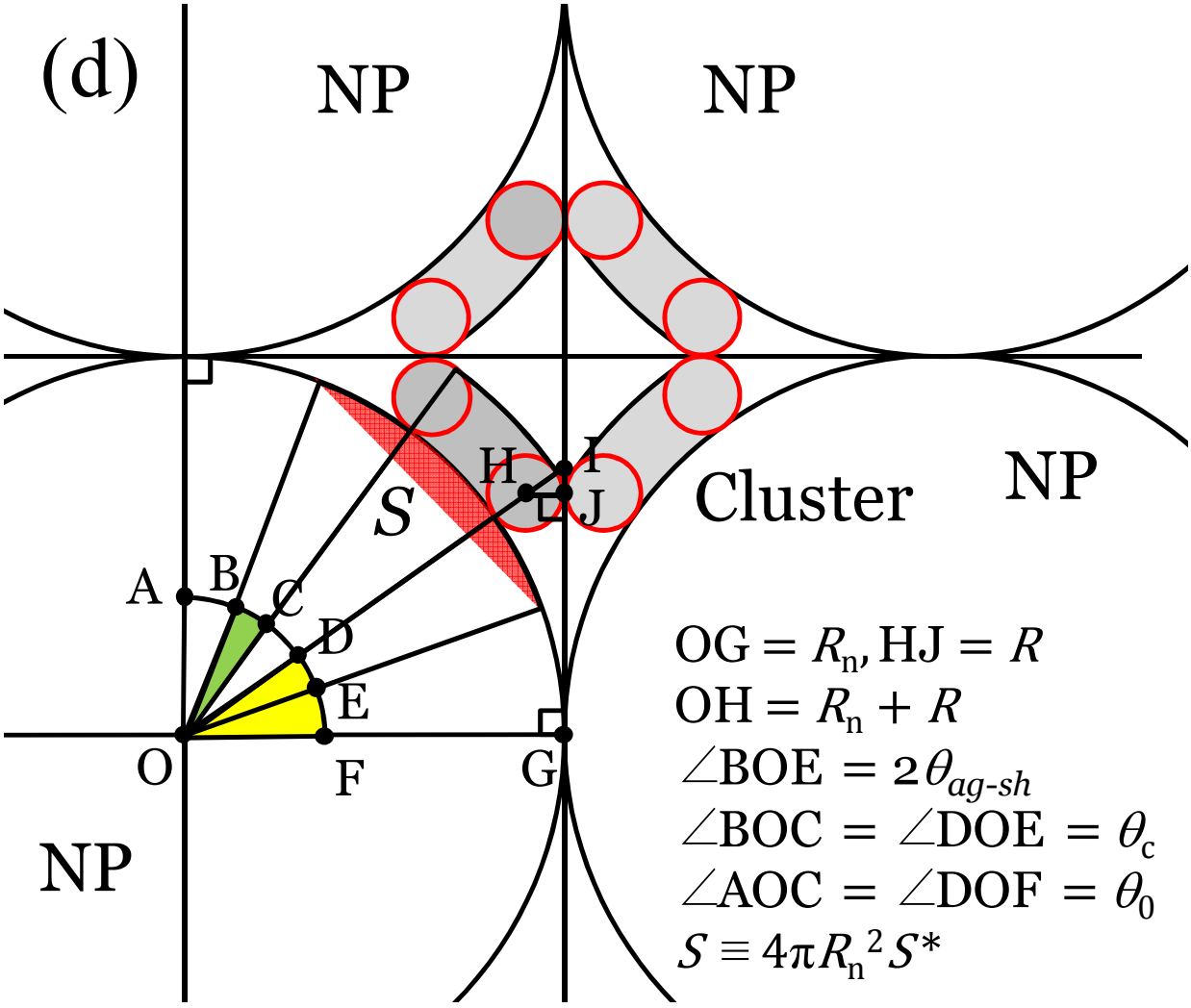

Fig. 4: Relative configurations of the NPs near the boundaries between the different assemblies. (a) clump-dispersed boundary. (b) string-clump boundary. (c) sheet-string boundary. (d) aggregate-sheet boundary. θ_{cl-d}, θ_{st-cl}, θ_{sh-st} and θ_{ag-sh} are the onset angles for each boundary. The grey regions show where the clusters are. The red regions highlight the inaccessible areas S. Finally, we use green to indicate the angle θ_c as defined in Fig. 1(a).

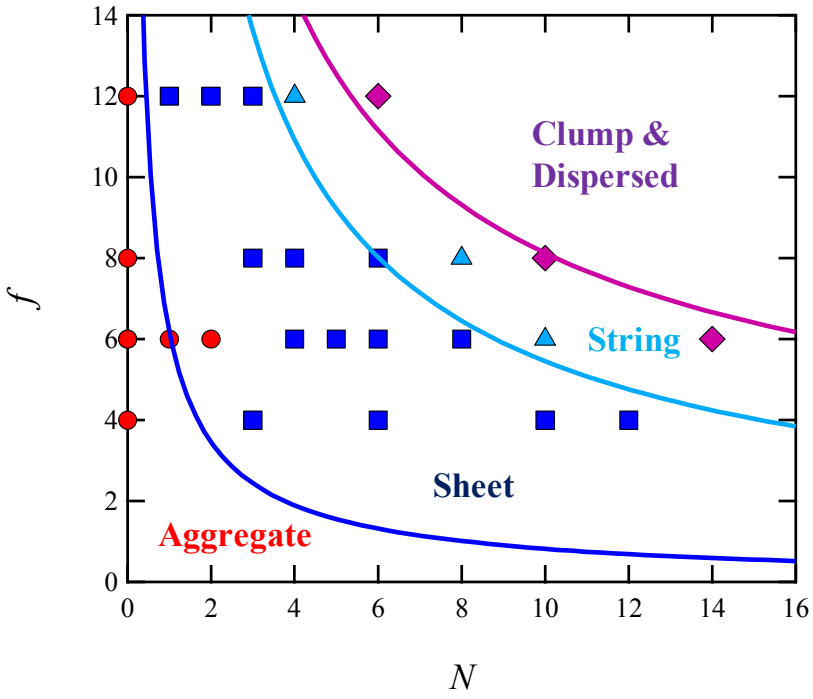

Fig. 5: Our theoretical phase boundaries (solid lines) plotted over the numerical phase diagram (symbols) obtained by Akcora et al.[1]. Note that in ref [1], a distinction between clumps and dispersed NPs was not indicated. We therefore categorized these two types of structures together as "clump & dispersed".